

**Empirical calculations of ^{29}Si NMR chemical shielding tensors:
A partial charge model investigation of hydrolysis in organically modified alkoxy silanes**

Todd M. Alam^a* and Marc Henry^b

RECEIVED
AUG 18 1999
OSTI

a Department of Aging and Reliability, Sandia National Laboratories, MS-1407, Albuquerque, NM 87185-1407, USA. E-mail:tmalam@sandia.gov

b Laboratoire de Chimie Moleculaire de l'Etat Solide, Universite Louis Pasteur, 67070 Strasbourg Cedex, France.

The ^{29}Si NMR chemical shifts for a series of organically modified silane compounds, $\text{Me}_x\text{Si}(\text{OR})_y(\text{OH})_{4-x-y}$ ($\text{OR} = \text{OMe}, \text{OEt}$), were evaluated using a partial charge model (PCM) approach to describe the chemical bonding. These PCM results allow the relative contributions of the diamagnetic and paramagnetic terms in the ^{29}Si NMR chemical shielding constant to be discussed. An explanation for the unique variations in the ^{29}Si chemical shifts during hydrolysis of organically modified silanes is presented.

* Corresponding author

DISCLAIMER

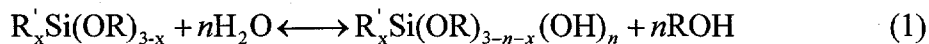
This report was prepared as an account of work sponsored by an agency of the United States Government. Neither the United States Government nor any agency thereof, nor any of their employees, make any warranty, express or implied, or assumes any legal liability or responsibility for the accuracy, completeness, or usefulness of any information, apparatus, product, or process disclosed, or represents that its use would not infringe privately owned rights. Reference herein to any specific commercial product, process, or service by trade name, trademark, manufacturer, or otherwise does not necessarily constitute or imply its endorsement, recommendation, or favoring by the United States Government or any agency thereof. The views and opinions of authors expressed herein do not necessarily state or reflect those of the United States Government or any agency thereof.

DISCLAIMER

**Portions of this document may be illegible
in electronic image products. Images are
produced from the best available original
document.**

1 Introduction

Organically modified alkoxy silanes play an important role in tailoring different properties of silica produced by the sol-gel method. Changes in the size and functionality of the organic group allows control of both physical and chemical properties of the resulting gel, with the kinetics of the polymerization process playing an important role in the design of new siloxane materials. High resolution ^{29}Si NMR has proven to be valuable tool for monitoring the polymerization reaction, and has been used to investigate a variety of organically modified alkoxy silane systems.¹⁻⁴ The initial steps of acid-catalyzed sol-gel polymerization are the hydrolysis and esterification (reverse of hydrolysis) reactions described by



The identification and quantification of the different hydrolysis species ($\text{R}_x\text{Si}(\text{OR})_{3-x-n}$) produced in eqn. (1) is important to understanding the initial steps of the sol-gel polymerization process. Recently it has been noted that the assignment of the high-resolution ^{29}Si NMR spectra for the resulting hydrolysis species in organically modified alkoxy silanes is complicated by upfield and/or downfield variations in the chemical shifts with hydroxyl addition.^{2,4-6} More complicated NMR experiments, including INEPT and DEPT based experiments have been used to correctly assign these different ^{29}Si NMR chemical shifts in simple organically modified alkoxy silanes.^{2,4,6-9} A basic understanding of what factors control the magnitude and sign of these chemical shift variations with hydroxyl addition remains unclear. The development of theoretical methods that would allow the assignment of ^{29}Si chemical shifts for the hydrolysis products for a wide range of organically modified

silanes based on some easily predicted property would prove valuable in future investigations. There have been a limited number of *ab initio* ^{29}Si chemical shift tensor calculations for simple silanes.¹⁰⁻¹³ Increases in the computational speed and efficiency suggest that *ab initio* calculations for silicon containing compounds will become more routine in the near future. Empirical methods have also been used to calculated ^{29}Si chemical shifts,^{14,15} including the use of partial charge models (PCM).¹⁶ The advantage of PCM methods is that the calculation of chemical shift for rather large molecular systems with limited computational expense. In this manuscript, we report the empirical PCM evaluation of the ^{29}Si chemical shifts in methyl substituted methoxy and ethoxy alkoxy silanes, $\text{Me}_x\text{Si}(\text{OR})_y(\text{OH})_{4-x-y}$ ($\text{OR} = \text{OMe, OEt}$). Using a structural dependent PCM the variations in the ^{29}Si chemical shift are directly related to changes in the partial charge, $q(\text{Si})$, on the silicon atom and the average excitation energy (ΔE) of the silane.

2 Experimental and computational methods

The silanes TEOS (Kodak), MTES (Aldrich), DMDES (Gelest), TMES (Gelest), TMOS (Aldrich), MTMS (Petrarch Systems), DMDMS (Gelest) and TMMS (Aldrich) were used as received without further purification. For each silane investigated a 2.24 M solution was prepared in the parent alcohol (MeOH or EtOH). The stock solution was analyzed for condensation and hydrolysis contaminants prior to use by ^{29}Si NMR. Hydrolysis species were generated by the addition of 3 molar equivalents of doubly distilled H_2O ($R_w = 3.0$). No acid or base catalysts were employed in these investigations to reduce condensation reactions during investigations.

All ^{29}Si NMR experiments were performed at 79.49 MHz on a Bruker AMX400 spectrometer, using a 5mm broadband probe at 298 ± 0.2 K. A DEPT pulse sequence was

used to assign the hydrolysis species in these investigations.¹⁷ The inter-pulse delay τ and the variable pulse angle θ in the DEPT experiment were optimized for the multiple heteronuclear Si-H couplings present in these silanes, as previously described.⁶ Chemical shifts were referenced to 0.1 % internal TMS ($\delta = 0.0$ ppm).

Empirical ²⁹Si chemical shift calculations were performed using the lab-developed PC software program WinPacha. Starting 3D-geometries were imported as Z-matrices in MOPAC format, and as a first approximation used standard bond-lengths and assumed tetrahedral symmetry around silicon. The charge distributions reported were computed assuming that the s-orbital participation to a chemical bond of an element having N_V valence electrons was $1/N_V$ ¹⁸ except for chlorine where a value of 25% seems to be more appropriate than the standard 14.3%. For the chemical hardnesses η the Bragg-Slater set of radii have been used, and provide a good measure of the spatial extent of the outer valence orbitals of the elements.¹⁹

3 Theoretical background

The NMR resonance frequency, ω , of a nucleus with gyromagnetic ratio γ placed in a static magnetic field, B_0 , is given by $\omega = \gamma B_0 (1 - \sigma)$. The nuclear magnetic shielding tensor σ measures the influence of the molecular environment on the apparent magnetic field observed at the nucleus, and shifts the observed NMR resonance from the frequency of a bare nucleus. It is often convenient to express the perturbation theory expansion of the chemical shielding tensor as a sum of a first-order (diamagnetic) term σ^d and a second-order (paramagnetic) term σ^p , both resulting from electronic currents localized on the atom containing the nucleus of interest.²⁰⁻²²

$$\sigma = \sigma^d + \sigma^p \quad (2)$$

The diamagnetic term contains only matrix elements involving the ground state wavefunctions, and can be expressed as:²³

$$\sigma^d = \left(\frac{\mu_0 e^2}{12\pi m_e} \right) \times \sum_{\gamma} P_{\gamma} \langle \gamma | \frac{1}{r_{\gamma}} | \gamma \rangle \quad (3)$$

where μ_0 is the vacuum permeability, e is the electron charge, m_e is the electron mass ($\mu_0 e^2 / 12\pi m_e = 9.39 \text{ ppm.}\text{\AA}$). P_{γ} is the charge density in the atomic orbital γ which is at an average distance of r_{γ} from nucleus of interest.

The paramagnetic contribution to the shielding tensor component σ^p is opposite in sign to σ^d , and involves unperturbed excited wave functions surrounding the nucleus. If a mean excitation energy ΔE is introduced,²⁴ then the individual shielding tensor elements (σ_{xx}^p , σ_{yy}^p and σ_{zz}^p) are defined by

$$\sigma_{ii}^p = - \left(\frac{\mu_0 \mu_B^2}{\pi a_0^3} \right) \times \frac{\langle (a_0 / r)^3 \rangle_{np}}{\Delta E} \times [P_{jj} + P_{kk} - P_{ij}P_{kk} + P_{jk}P_{kj}] \quad i, j, k = x, y, z \quad (4)$$

where P_{ij} is the charge distribution and bond order matrix, $\langle r^{-3} \rangle_{np}$ the average electron-nucleus distance r over p-orbitals, μ_B the Bohr magneton and a_0 the Bohr radius ($\mu_0 \mu_B^2 / \pi a_0^3 = 1449 \text{ ppm.eV}$). For the isotropic ²⁹Si NMR chemical shieldings reported in the results section, only the rotational average of the individual tensor elements in eqn. (4) are observed, producing an isotropic paramagnetic shielding defined by

$$\sigma_{iso}^p = \frac{1}{3}(\sigma_{xx}^p + \sigma_{yy}^p + \sigma_{zz}^p) = -\frac{2}{3} \left(\frac{\mu_0 \mu_B^2}{\pi a_0^3} \right) \times \frac{\langle (a_0/r)^3 \rangle_{np}}{\Delta E} \times P_u \quad (5)$$

where P_u is the population unbalance, and measures the deviation from spherical symmetry of the electronic cloud defined by

$$P_u = (P_{xx} + P_{yy} + P_{zz}) - \frac{1}{2}(P_{xx}P_{zz} + P_{yy}P_{xx} + P_{yy}P_{zz}) + \frac{1}{2}(P_{xy}P_{yx} + P_{xz}P_{zx} + P_{zy}P_{yz}) \quad (6)$$

The changes in the observed ^{29}Si chemical shielding result from the fine balance between four terms σ^d , $\langle r^{-3} \rangle_{np}$, ΔE and P_u . The first two terms, σ^d and $\langle r^{-3} \rangle_{np}$, are functions of the gross atomic population $N = P_s + P_{xx} + P_{yy} + P_{zz}$ and can be related to the partial atomic charge on silicon $q(\text{Si}) = Z - N$. The last two terms ΔE and P_u are generally obtained from molecular orbital theory, but have also been shown to be dependent on the silicon partial atomic charge $q(\text{Si})$.¹⁶ A reliable way of estimating these partial atomic charges is important for the subsequent analysis of chemical shifts trends.

3.1 The partial charge model (PCM) approach of chemical bonding

The identification of the electronegativity χ as the opposite of the electronic chemical potential μ_e ($\chi = -\mu_e$),²⁵ and of the chemical hardness η to the HOMO-LUMO energy gap,²⁶ allows a straightforward and reliable evaluation of partial atomic charges q independently of any molecular orbital calculations. From a practical point of view, given any system resulting

from the association of n atoms, with a total electrical charge Z , it is possible to write the system electronegativity as:²⁷

$$\chi_i = \langle \chi \rangle = \chi_i^0 + \frac{e}{4\pi\epsilon_0 r_i} q_i + \frac{1}{4\pi\epsilon_0} \sum_{j=1}^n \frac{eq_j}{R_{ij}} \quad \forall i = 1, \dots, n \quad \text{with} \quad \sum_{i=1}^n q_i = Z \quad (7)$$

where ϵ_0 the vacuum permittivity, χ_i^0 are Mulliken electronegativities of the valence orbitals used for chemical bonding,¹⁸ r_i the atomic radii modelling the spatial extent of these orbitals and R_{ij} is the distance between atoms i and j in the compound with partial charge q_i . Equation (7) allows a set of chemical parameters (electronegativities, sizes and atomic spatial positions), and the associated partial charge distribution q_i to be easily related thereby allowing relationships between chemical shielding and partial charge to be established.

Using the PCM, the diamagnetic shielding described by eqn. (3) is calculated taking in account the partial charge distribution and the polynomial approximation of Saxena and Narasimhan for a ²⁹Si nucleus bearing a partial charges $q(\text{Si})$.²⁸ The diamagnetic shielding is then given by^{23,29}

$$\sigma^d = \sigma^d(\text{free atom}) + \left(\frac{\mu_0 e^2}{12\pi m_e} \right) \sum_N \left(\frac{Z_N}{r_N} \right) \quad (8)$$

where σ^d (free atom) is the free atom diamagnetic susceptibility, Z_N is the atomic number of atom N , r_N is the distance from the nucleus of interest and atom N , and the summation runs over all atoms directly attached to the atom of interest.

For the evaluation of the paramagnetic shielding in eqn. (5) the radial term $\langle a_0 / r^3 \rangle_{np}$ is known to vary with the partial charge $q(\text{Si})$ as

$$\langle (a_0 / r)^3 \rangle_{np} = \langle (a_0 / r)^3 \rangle_{np}^0 + f \times q(\text{Si}) = R_0 + f \times q(\text{Si}) \quad (9)$$

where f is a adjustable parameter close to unity. Fortunately, PCM gives us not only the partial charge at the silicon $q(\text{Si})$, but also the partial charges on all of the surrounding nuclei thus allowing the anisotropy of the charge to be determined. The charge deviation (Δq) from the average isotropic charge and the deviation from axial symmetry (δq) are defined by

$$\Delta q = |q_i|_{\max} - \sum_{i=1}^4 |q_i| / 4 \quad (10a)$$

$$\delta q = |q_j|_{j \neq i}^{\max} - \sum_{k \neq i, j} |q_k| / 2 \quad (10b)$$

Assuming that the silicon atom forms four molecular orbitals using one s - and three p -orbitals, charge conservation requires

$$P_s + P_{xx} + P_{yy} + P_{zz} = 4 - q(\text{Si}) \quad (11)$$

The charge and charge deviation can be related to the orbital populations by

$$P_{xx} = 1 - [q(\text{Si}) + q_s(\text{Si}) + \Delta q + \delta q] / 3 \quad (12a)$$

$$P_{yy} = 1 - [q(\text{Si}) + q_s(\text{Si}) + \Delta q] / 3 \quad (12b)$$

$$P_{zz} = 1 - (q(\text{Si}) + q_s(\text{Si}) - 2\Delta q - \delta q) / 3 \quad (12c)$$

where $q_s(\text{Si}) = 1 - P_s$.

From these relationships P_u and $\langle a_0 / r^3 \rangle_{np}$ are directly related to the silicon partial charge $q(\text{Si})$. The main obstacle remaining is the evaluation of the ΔE parameter, whose values can have a substantial influence on the paramagnetic contribution. The approach outlined in this manuscript entails the initial optimization the parameters R_0, f and ΔE using a standard set of reference molecules for which structures and absolute ^{29}Si chemical shielding values are known. The remaining parameters in eqns. (2-12), σ^d , $q(\text{Si})$ and $q_s(\text{Si})$, are fixed by molecular geometry and the assumptions about the electronegativity and hardness of the atoms. Fixing these parameters obtained for the reference compounds allows the ^{29}Si chemical shifts for the remaining alkoxy silane species investigated to be directly evaluated.

4. Results and Discussion

The ^{29}Si NMR chemical shifts for the organically modified silane compounds, $\text{Me}_x\text{Si}(\text{OR})_{4-x}$ ($\text{OR} = \text{OMe}, \text{OEt}$) under different solution conditions is shown in Table 1. Chemical shifts (with respect to internal TMS) increase from approximately +0.2 to +2 ppm on going from a neat alkoxy solution to a 2.24 M solution in the parent alcohol. The symmetric TEOS and TMOS compounds show the smallest variation with only a +0.2 to +0.25 ppm increase. After the addition of three equivalents of water ($R_w = 3.0$) to the stock solution (and prior to extensive condensation) an additional increase in the ^{29}Si chemical shift of approximately + 1 ppm was observed for the entire series, except TEOS and TMOS where only a $\sim +0.2$ ppm variation was observed. These changes in the ^{29}Si NMR chemical shifts clearly justify the importance of defining the solution conditions during NMR investigations where the

magnitude of chemical shift variations due to solvent composition are comparable to the differences produced by hydrolysis. In the work described here, this is the situation encountered, where the observed chemical shift dispersion due to hydrolysis of methyl modified alkoxy silanes is very small and could be easily masked by changes in the composition of the solution. Due to the influence of the solvent, the chemical shifts for the methyl alkoxy silane series were all obtained under identical conditions of 2.24 M and $R_w = 3.0$. This strong solvent dependence also precludes the direct comparison of ^{29}Si NMR chemical shifts previously reported in literature. The ^{29}Si NMR chemical shifts for the $\text{Me}_x\text{Si}(\text{OR})_y(\text{OH})_{4-x-y}$ ($\text{OR} = \text{OMe}, \text{OEt}$) series are listed in Table 2. The use of consistent solution conditions allows the variation of the chemical shift ($\Delta\delta$) with each OH functional group incorporated into the alkoxy silane during hydrolysis to be directly compared, and are given in Table 2.

Figure 1 shows the correlation between $\Delta\delta$ and the number of attached hydroxyl groups for compounds with differing number of attached methyl groups in both the methoxy and ethoxy silanes. For the unmodified alkoxy silanes, $\text{Si}(\text{OR})_y(\text{OH})_{4-y}$ ($\text{OR} = \text{OMe}, \text{OEt}$), a positive increase in the chemical shift was observed for each OH group added during hydrolysis. For the ethoxy series an increase of $\sim +2$ to $+3$ ppm was observed for each hydroxyl group, while for the methoxy series a slightly smaller shift of $\sim +1$ to $+2$ ppm per hydroxyl group was observed. For the single methyl-modified ethoxy series, ($x = 1$) $\text{Me}_x\text{Si}(\text{OEt})_y(\text{OH})_{4-x-y}$, variations of approximately $+1.2$ to $+1.7$ ppm shift per hydroxyl group were observed, while for the methyl-modified methoxy series ($x = 1$) $\text{Me}_x\text{Si}(\text{OMe})_y(\text{OH})_{4-x-y}$ both positive and negative shifts on the order of ± 0.1 to ± 0.2 ppm per hydroxyl group were observed. Both positive and negative chemical shift variations with hydroxyl substitution were also observed for the dimethyl-substituted series, ($x = 2$) $\text{Me}_x\text{Si}(\text{OEt})_y(\text{OH})_{4-x-y}$. For the

trimethyl-substituted ethoxy silanes, ($x = 3$) $\text{Me}_x\text{Si(OEt)}_y(\text{OH})_{4-x-y}$, and the di- and trimethyl-substituted methoxy silanes, ($x = 2$ or 3) $\text{Me}_x\text{Si(OMe)}_y(\text{OH})_{4-x-y}$, negative chemical shift variations of approximately -3 to -6 ppm per hydroxyl group were observed. As seen in Fig. 1 the addition of hydroxyl groups can produce both negative and positive variations in the chemical shifts depending on the number of methyl substituents attached to the silicon, as well as the identity of the alkoxy group. An explanation of these trends based on semi-empirical predictions of the ^{29}Si chemical shift are detailed below.

4.1 PCM calibration

The theory section detailed the semi-empirical PCM procedure to predict the diamagnetic shielding (eqn. 3) and the paramagnetic shielding (eqn. 6). To calibrate and validate eqns. (2-12), the ^{29}Si NMR chemical shielding constants for a set of reference molecules, for which shielding constants and molecular structure are known, were evaluated. Previously the absolute ^{29}Si chemical shielding for SiH_4 ($\sigma^0 = 475.3 \pm 10$ ppm), SiF_4 ($\sigma^0 = 482 \pm 10$ ppm), SiCl_4 ($\sigma^0 = 384.15 \pm 10$ ppm), SiMe_4 ($\sigma^0 = 368.5 \pm 10$ ppm) and SiO_2 (quartz) ($\sigma^0 = 475.90 \pm 10$ ppm) have been reported.³⁰ In addition the chemical shielding for the symmetric compounds $\text{Si}(\text{OH})_4$, $\text{Si}(\text{OMe})_4$ and $\text{Si}(\text{OEt})_4$ reported in this study (Table 1) were included in the original parameterization of the PCM model.

Based on the molecular geometries of these reference compounds, the partial charge on silicon $q(\text{Si})$ were easily calculated using PCM. As a first approximation the mean excitation energy ΔE used in eqn. (6) is confined between the lowest U.V. absorption band and the ionization potential of the investigated compounds. If eqns. (2-12) are correct the absolute shielding constants of these reference compounds should be reproduced with just

three adjustable parameters: ΔE , R_0 and f , while the remaining parameters, σ_{dia} , $q(\text{Si})$ and $q_s(\text{Si})$, are directly determined by the geometry and the assumptions about the electronegativities and hardness of the atoms. In fact once, R_0 and f are known or fixed, eqn. (6) can be easily inverted to obtain the ΔE values from the experimental shielding constants.

Table 3 shows the populations of silicon outer-valence orbitals deduced from PCM for these reference compounds. As expected, the s-orbital population (P_s) was found to be higher with good electron-donors ligands such as H^- , CH_3^- , O_2^{2-} , MeO^- and EtO^- and significantly lower with more electronegative ligands such as F^- , Cl^- and OH^- . Using these PCM populations and a simplex optimization, a minimum in the average error between theory and experiment ^{29}Si chemical shielding of 0.2 ppm was obtained for $R_0 = 3.277$, $f = 3.155$ and the corresponding ΔE values presented in Table 4.

Figure 2 shows that the average excitation energies, ΔE , vary rather smoothly with partial charge $q(\text{Si})$. The typical U-shaped curve obtained is not unexpected from a theoretical point of view, and has been noted before.¹⁶ Figure 2 also provides an explanation for the quite surprising experimental observation that SiH_4 and SiF_4 , which have very different electronic structures, nevertheless have very similar shielding constants. The basis for the similar ΔE values in these two compounds arises from the fact that for SiH_4 , ΔE is approximates the HOMO-LUMO gap, whereas for SiF_4 ΔE is more accurately described by the energy difference in atomic orbitals.

The strong deshielding experimentally observed for TMS relative to SiH_4 or SiCl_4 relative to SiF_4 (Table 4) is also a direct consequence of the U-shaped dependence of ΔE on $q(\text{Si})$. From Fig. 2, these two pairs of molecules are located on opposite branches of the $\Delta E - q(\text{Si})$ correlation with the reduced ΔE value observed for TMS reflecting a more polar covalent bond, and for SiCl_4 a more covalent polar bond. For Si-O bonds the polarities are

intermediate between SiCl_4 and SiF_4 . This results in compounds containing SiO_4 units being shielded relative to TMS or SiCl_4 , and deshielded relative to SiF_4 . The regular increase in ΔE observed in the series $\text{Si(OEt)}_4 \rightarrow \text{Si(OMe)}_4 \rightarrow \text{Si(OH)}_4 \rightarrow \text{SiO}_2$ is easily understandable in terms of the mean electronegativities $\langle \chi \rangle$ of the ligands attached to silicon: $\text{OEt} = 8.10 > \text{OMe} = 8.35 > \text{OH} = 9.23 > \text{O} = 12.56$, as this parameter is a direct measure of the Fermi level of the electrons in the compounds.

4.2 PCM Analysis of ^{29}Si Chemical Shielding

A similar analysis of ^{29}Si shielding tensors can be performed for the series, $\text{Me}_x\text{Si(OR)}_y(\text{OH})_{4-x-y}$ ($\text{OR} = \text{OMe}$, OEt). From PCM analysis the gross populations of the outer valence orbitals can be determined and are given in Table 5. Fixing the radial parameters to the values obtained for the reference compounds, $R_0 = 3.277$ and $f = 3.155$, the experimentally observed ^{29}Si shielding constants can be reproduced by variation of a single adjustable parameter ΔE . The resulting parameters following optimization are shown in Table 6. As a check of the quality of these optimized values, Figure 3 shows the variation of ΔE versus the partial charge on silicon $q(\text{Si})$. The smooth variation between ΔE and $q(\text{Si})$ observed suggests that the approximations utilized are relatively good. This relationship between ΔE and $q(\text{Si})$ can be used to predict ^{29}Si chemical shifts for other organically modified alkoxy silanes based on the determination of $q(\text{Si})$. PCM also allows an estimate of the chemical shielding anisotropy (CSA). As shown in Table 6, predicted CSA values range between 0 and 60 ppm, with a mean value of 39 ppm computed for the unsymmetrical silanes. Fortunately, ^{29}Si chemical shielding parameters have been reported in literature for the three compounds $\text{Me}_3\text{Si(OMe)}$ ($\Delta\sigma = 40$ ppm, $\eta = 0.08$), $\text{Me}_2\text{Si(OMe)}_2$ ($\Delta\sigma = 47$ ppm, $\eta = 0$) and MeSi(OMe)_3 ($\Delta\sigma = 39$ ppm, $\eta = 0.46$). {Gibby, 1972 #32} While the agreement is not perfect, the right order of

magnitude and experimental trends are correctly predicted for $\Delta\sigma$ ($\Delta\sigma[\text{SiX}_3\text{Y}] \sim \Delta\sigma[\text{SiY}_3\text{X}] < \Delta\sigma[\text{SiX}_2\text{Y}_2]$). This observation also supports the PCM semi-empirical method.

The goodness of the fit between experimental and theoretical ^{29}Si chemical shielding is shown in Figure 4, where the correlation of fit was $r^2 = 0.9998$ and an average error of 0.5 ppm for the isotropic shielding constants. This excellent agreement again supports the parameterization and allows insight into balance between σ^d , $\langle (a_0 / r)^3 \rangle_{np}$, ΔE and P_u in these compounds. From these results, it is clear that the deshielding observed during TEOS or TMOS hydrolysis results from the interplay between shielding action of the ΔE term and its ability to cancel the conjugate deshielding action of σ^d and $\langle (a_0 / r)^3 \rangle_{3p}$. This leaves the deshielding contribution from the increase in P_u as an important factor for the observed chemical shift variations in the $\text{Si}(\text{OEt})_{4-x}(\text{OH})_x$ and $\text{Si}(\text{OMe})_{4-x}(\text{OH})_x$ series. Table 5 shows that when electronegative OH groups replace less electronegative ethoxy groups, the silicon s-orbital populations are more affected than the p-orbitals. It is this preferential overlap of OH groups with the silicon s-orbital which is responsible for the increased population unbalance (P_u) in the p-orbital, thus producing the deshielding of the ^{29}Si nucleus with hydrolysis of TEOS or TMOS. The methoxy group is more electronegative than the ethoxy substituent, with the P_u variation being accordingly reduced. This increase in electronegativity explains the reduced chemical shift range observed for TMOS hydrolysis species relative to TEOS hydrolysis species. A similar argument is observed for the $\text{MeSi}(\text{OEt})_{3-x}(\text{OH})_x$ series, with the reduced variation in P_u producing smaller deshielding effects than in TEOS.

In the $\text{MeSi}(\text{OMe})_{3-x}(\text{OH})_x$ and $\text{Me}_2\text{Si}(\text{OEt})_{2-x}(\text{OH})_x$ series, there is nearly an equal compensation between the deshielding action of the $\langle (a_0 / r)^3 \rangle_{3p}$ term and the shielding action of the ΔE . In these compounds the changes in the P_u term can now produce either relative

shielding or deshielding of the ^{29}Si nucleus. The almost exact balance of these terms leads to a small observed chemical shift variations. For the limited $\text{Me}_3\text{Si}(\text{OEt})_{1-x}(\text{OH})_x$, $\text{Me}_2\text{Si}(\text{OMe})_{2-x}(\text{OH})_x$ and $\text{Me}_3\text{Si}(\text{OMe})_{1-x}(\text{OH})_x$ series there is either a very small change or an increase in the diamagnetic shielding with hydroxyl addition, plus a shielding effect of the decreasing P_u term. These decreases in the orbital unbalance suggest that with substitution of the electronegative OH group for ethoxy or methoxy, the effect on the population of p- and s-orbitals are very similar in silanes with higher number of methyl substitutions. In general the chemical shifts observed for the hydrolysis of these modified silanes is dominated by the population unbalance P_u , with the effects of the $\langle (a_0 / r)^3 \rangle_{3p}$ and ΔE nearly balancing the negligible changes in σ^d .

A different picture emerges from the analysis of the $\text{Me}_x\text{Si}(\text{OR})_{4-x}$ series. In this series the $\langle (a_0 / r)^3 \rangle_{3p}$ and ΔE terms still produce opposite effects, but the radial term produces a shielding trend as the partial charge on silicon $q(\text{Si})$ decreases with increasing x , while ΔE produces a deshielding effect as it decreases with increasing x . The diamagnetic contribution σ^d is no longer negligible and has a constant deshielding effect. In addition, the P_u contribution is high for oxygen-rich compounds and tends to be low for carbon-rich ones. With the combination of these effects, the result is a deshielding trend with increasing x , except for the end of the series Me_3SiOR and TMS. In that case the high shielding effect resulting from the large decrease in $q(\text{Si})$ produced by removing the last oxygen, and cannot be compensated by the very modest ΔE and P_u variations. This same effect gives rise to the well-known "sagging pattern" of ^{29}Si NMR shielding in $\text{R}_x\text{SiX}_{4-x}$ series where R is an alkyl group and X an electronegative substituent.

An important conclusion from this study, is that the $\langle (a_0 / r)^3 \rangle_{3p}$ and ΔE terms tend to cancel each other, leaving the domination of the paramagnetic shielding to the orbital unbalance P_u term. It was also demonstrated that it is not the absolute values of the R_0, f or ΔE parameters which are important, but rather the correlation in the p-orbitals expansion to increases or decreases in ΔE . These two parameters, $\langle (a_0 / r)^3 \rangle_{3p}$ and ΔE cannot be varied in an independent way, but instead are strongly related. As in previous work done on ^{29}Si NMR shielding constants, the so-called "average excitation energy" approximation is surely a very good one, but the concept of a "constant average excitation energy" is not sufficient. Instead the ^{29}Si chemical shielding can be better approximated by maintaining a constant $\langle (a_0 / r)^3 \rangle_{3p} / \Delta E$ ratio.

Acknowledgement

This work was partially supported (TMA) by the Basic Energy Science (BES) program at Sandia National Laboratories. Sandia is a multiprogram laboratory operated by Sandia Corporation, a Lockheed Martin Company, for the U. S. Department of Energy under Contract No. DE-AC04-94AL8500.

References

- 1 R. J. Hook, *J. Non-Cryst. Solids*, 1996, **195**, 1.
- 2 T. M. Alam; R. A. Assink; D. A. Loy, *Chem. Mater.*, 1996, **8**, 2366.
- 3 Y. Sugahara; T. Inoue; K. Kuroda, *J. Mater. Chem.*, 1997, **7**, 53.
- 4 F. Brunet, *J. Non-Cryst. Solids*, 1998, **231**, 58.
- 5 T. M. Alam; R. A. Assink; S. Prabakar; D. A. Loy, *Magn. Reson. Chem.*, 1996, **34**, 603.
- 6 T. M. Alam, *Spectrochimica Acta Part A*, 1997, **53**, 545.
- 7 P. Lux; F. Brunet; H. Desvaux; J. Virlet, *J. Chim. Phys.*, 1994, **91**, 409.
- 8 P. Lux; F. Brunet; J. Virlet; B. Cabane, *Magn. Reson. Chem.*, 1996, **34**, 100.
- 9 P. Lux; F. Brunet; J. Virlet; B. Cabane, *Magn. Reson. Chem.*, 1996, **34**, 173.
- 10 J. F. Hinton; P. L. Guthrie; P. Pulay; K. Wolinski, *J. Magn. Reson.*, 1993, **103**, 188.
- 11 D. Cremer; L. Olsson; H. Ottosson, *J. Molec. Struct. (Theochem)*, 1994, **313**, 91.
- 12 H. Nakatsuji; T. Nakajima; M. Hada; H. Takashima; S. Tanaka, *Chem. Phys. Letts.*, 1995, **247**, 418.
- 13 R. Wolff; R. Radeglia, *J. Molec. Structure (Theochem)*, 1994, **313**, 111.
- 14 D. Kovacek; Z. B. Maksic; S. Elbel; J. Kudnig, *J. Molec. Structure (Theochem)*, 1994, **304**, 247.
- 15 G. Englehardt; R. Radeglia; H. Jancke; E. Lippmaa; M. Mägi, *Organ. Magn. Reson.*, 1973, **5**, 561.
- 16 M. Henry; C. Gerardin; F. Taulelle *Electronegativity-Based Computation of ²⁹Si Chemical Shifts*; M. Henry; C. Gerardin; F. Taulelle, Ed.; Materials Research Society: San Francisco, CA, 1992; Vol. 271, pp 243.
- 17 D. T. Pegg; D. M. Doddrell; M. R. Bendall, *J. Chem. Phys.*, 1982, **77**, 2745.

18 S. G. Bratsch, *J. Chem. Educ.*, 1988, **65**, 34.

19 J. C. Slater, *J. Chem. Phys.*, 1964, **41**, 3199.

20 M. Karplus; T. P. Das, *J. Chem. Phys.*, 1961, **34**, 1683.

21 A. Abragam, in *Principles of Nuclear Magnetism*, ed. Adair, R. K., Elliot, R. J., Marshall, W. C. and Wilkinson, D. H., Clarendon Press, Oxford, 1961, 599.

22 A. Carrington; A. D. McLachlan, in *Introduction to Magnetic Resonance*, ed. Rice, S. A., Harper & Row, New York, 1967, 266.

23 W. H. Flygare; J. Goodisman, *J. Chem. Phys.*, 1968, **49**, 3122.

24 A. Velenik; R. M. Lynden-Bell, *Mol. Phys.*, 1970, **19**, 371.

25 R. G. Parr; R. A. Donnelly; M. Levy; W. E. Palke, *J. Chem. Phys.*, 1978, **68**, 3801.

26 R. G. Pearson, *Coordination Chem. Reviews*, 1990, **100**, 403.

27 M. Henry, *Coordination Chem. Reviews*, 1998, **170-180**, 1109.

28 K. M. S. Saxena; P. T. Narasimhan, *Internal. J. Quant. Chem.*, 1967, **1**, 731=749.

29 W. B. Moniz; C. F. Poranski, *J. Magn. Reson.*, 1973, **11**, 62.

30 C. J. Jameson; A. K. Jameson, *Chem. Phys. Letts.*, 1988, **149**, 300.

31 The fourth order polynomial, $\Delta E = \sum_{n=0}^3 a_n \cdot q(Si)^n$ where $a_0 = 8.155$, $a_1 = -3.03$, $a_2 = 24.64$ and $a_3 = -28.48$ is shown.

Figures

Fig. 1 Changes of the chemical shift variation ($\Delta\delta$) with number of attached hydroxyls (n_{H_2O} = 4-x-y) in the alkoxy silane series a) $Me_xSi(OEt)_y(OH)_{4-x-y}$ and b) $Me_xSi(OMe)_y(OH)_{4-x-y}$. Note that the addition of hydroxyl groups produces both positive and negative variations in the chemical shift versus the non-hydrolyzed alkoxy silanes.

Fig. 2 Correlation between the average excitation energy (ΔE) and the partial charge on the silicon atom $q(Si)$ for the eight reference compounds given in Table 4. A fourth order polynomial curve is shown for visual reference.

Fig. 3 Correlation between the average excitation energy (ΔE) and the partial charge on the silicon atom $q(Si)$ for the alkoxy silane series $Me_xSi(OR)_y(OH)_{4-x-y}$ (R = Me, Et). A fourth order polynomial is given for visual reference.³¹

Fig. 4 The correlation between the observed chemical shielding (σ_{exp}) and the theoretically predicted chemical shielding (σ_{theory}) using the PCM model. The correlation of linear fit $r^2 = 0.9998$ was obtained.

Table 1 ^{29}Si NMR isotropic chemical shifts for methyl modified alkoxy silanes under different solution conditions^a

Silane ^c	Neat ^b	2.24 M ^b	$R_w = 3.0^b$
TEOS	-82.22	-81.97	-81.82
MTES	-44.06	-43.27	-42.14
DMDES	-5.57	-4.14	-3.85
TMES	+14.66	+16.71	+17.78
TMOS	-78.81	-78.55	-78.29
MTMS	-40.11	-39.46	-38.24
DMDMS	-1.98	+0.41	+1.25
TMMS	+17.32	+19.52	+20.72

^a All chemical shifts referenced to internal tetramethylsilane, TMS (0.1%).

^b Solution composition: Neat = silane plus reference TMS (0.1%), 2.24 M = silane concentration in parent alcohol, $R_w = 3.0$ is 2.24 M solution plus 3 molar equivalents of distilled H₂O added.

^c TEOS, tetraethoxysilane; MTES, methyltriethoxysilane; DMDES, dimethyldimethoxysilane; TMES, trimethylethoxysilane; TMOS, tetramethoxysilane; MTMS, methyltrimethoxysilane; DMDMS, dimethyldimethoxysilane; TMMS, trimethyltrimethoxysilane.

Table 2 ^{29}Si NMR chemical shifts and absolute chemical shieldings (ppm) of methyl modified alkoxy silane solutions ^a

Silane	δ (ppm) ^b	σ (ppm) ^c	$\Delta\delta$ ^d
Si(OEt)_4	-81.82	450.32	--
$\text{Si(OEt)}_3(\text{OH})$	-78.88	447.38	+2.94
$\text{Si(OEt)}_2(\text{OH})_2$	-76.45	444.95	+5.37
$\text{Si(OEt)}(\text{OH})_3$	-74.34	442.84	+7.48
Si(OH)_4	-72.43	440.93	+9.39
MeSi(OEt)_3	-42.14	410.64	--
$\text{MeSi(OEt)}_2(\text{OH})$	-40.43	408.93	+1.71
$\text{MeSi(OEt)}(\text{OH})_2$	-39.03	407.53	+3.11
MeSi(OH)_3	-37.85	406.35	+4.29
$(\text{Me})_2\text{Si(OEt)}_2$	-3.85	372.35	--
$(\text{Me})_2\text{Si(OEt)}(\text{OH})$	-3.41	371.91	+0.44
$(\text{Me})_2\text{Si(OH)}_2$	-4.17	372.67	-0.32
$(\text{Me})_3\text{Si(OEt)}$	17.78	386.28	--
$(\text{Me})_3\text{Si(OH)}$	14.60	383.10	-3.18
Si(OMe)_4	-78.29	446.79	--
$\text{Si(OMe)}_3(\text{OH})$	-76.03	444.53	+2.26
$\text{Si(OMe)}_2(\text{OH})_2$	-74.46	442.96	+3.83
$\text{Si(OMe)}(\text{OH})_3$	-73.22	441.72	+5.07
Si(OH)_4	-72.21	440.71	+6.08
MeSi(OMe)_3	-38.24	406.74	--
$\text{MeSi(OMe)}_2(\text{OH})$	-38.11	406.61	+0.13
$\text{MeSi(OMe)}(\text{OH})_2$	-38.13	406.63	+0.11
MeSi(OH)_3	-38.43	406.93	-0.19
$(\text{Me})_2\text{Si(OMe)}_2$	1.25	367.25	--
$(\text{Me})_2\text{Si(OMe)}\text{OH}$	-1.46	369.96	-2.71
$(\text{Me})_2\text{Si(OH)}_2$	-4.05	372.55	-5.30
$(\text{Me})_3\text{Si(OMe)}$	20.72	389.22	--
$(\text{Me})_3\text{Si(OH)}$	14.84	383.34	-5.88

^a2.24 M solutions, $R_w = 3.0$, 298 K. ^bAll chemical shifts internally referenced to TMS (0.1%).

^cChemical shielding values calculated assuming a $\sigma = 386.5$ ppm for TMS.³⁰

^d $\Delta\delta$ is the relative chemical shift with respect to the unhydrolyzed monomer species.

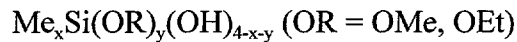
Table 3 Predicted PCM populations of silicon outer-valence orbitals for the reference compounds

Compound	P_s	P_{xx}	P_{yy}	P_{zz}	ΔP^a	P_u^b
$\text{Si}(\text{CH}_3)_4$	1.32852	0.85032	0.85032	0.85032	0.00000	0.97760
SiF_4	0.97020	0.57321	0.57321	0.57321	0.00000	0.81785
SiH_4	1.35414	0.88502	0.88502	0.88502	0.00000	0.98678
SiCl_4	1.06214	0.76977	0.76977	0.76977	0.00000	0.94699
SiO_2 (quartz)	1.27571	0.57679	0.57679	0.57679	0.00000	0.82089
$\text{Si}(\text{OH})_4$	1.11167	0.65689	0.65684	0.65727	0.00041	0.88235
$\text{Si}(\text{OCH}_3)_4$	1.24914	0.64468	0.64468	0.64468	0.00000	0.87375
$\text{Si}(\text{OC}_2\text{H}_5)_4$	1.28161	0.63562	0.63487	0.63977	0.00453	0.86805

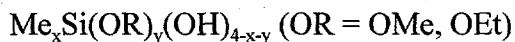
^a $\Delta P = P_{zz} - \frac{1}{2}(P_{xx} + P_{yy})$. ^b P_u defined by eqn. (7).

Table 4 ^{29}Si NMR shielding constants and corresponding parameters for reference compounds

Compound	σ_{exp} (ppm)	σ_{iso} (ppm)	σ_{dia} (ppm)	$q(\text{Si})$	ΔE (eV)
$\text{Si}(\text{CH}_3)_4$	368.50	368.51 (+0.01)	1008.13	0.121	8.10
SiF_4	482.00	481.68 (-0.32)	1094.56	1.310	14.33
SiH_4	475.30	475.18 (-0.12)	913.33	-0.009	10.60
SiCl_4	384.15	384.30 (+0.15)	1195.34	0.629	8.90
SiO_2 (quartz)	475.90	476.31 (+0.41)	1072.28	0.994	12.80
$\text{Si}(\text{OH})_4$	440.82	440.64 (-0.18)	1066.87	0.917	12.60
$\text{Si}(\text{OCH}_3)_4$	447.31	447.20 (-0.11)	1067.98	0.817	11.94
$\text{Si}(\text{OC}_2\text{H}_5)_4$	450.72	450.82 (+0.10)	1068.28	0.808	11.87

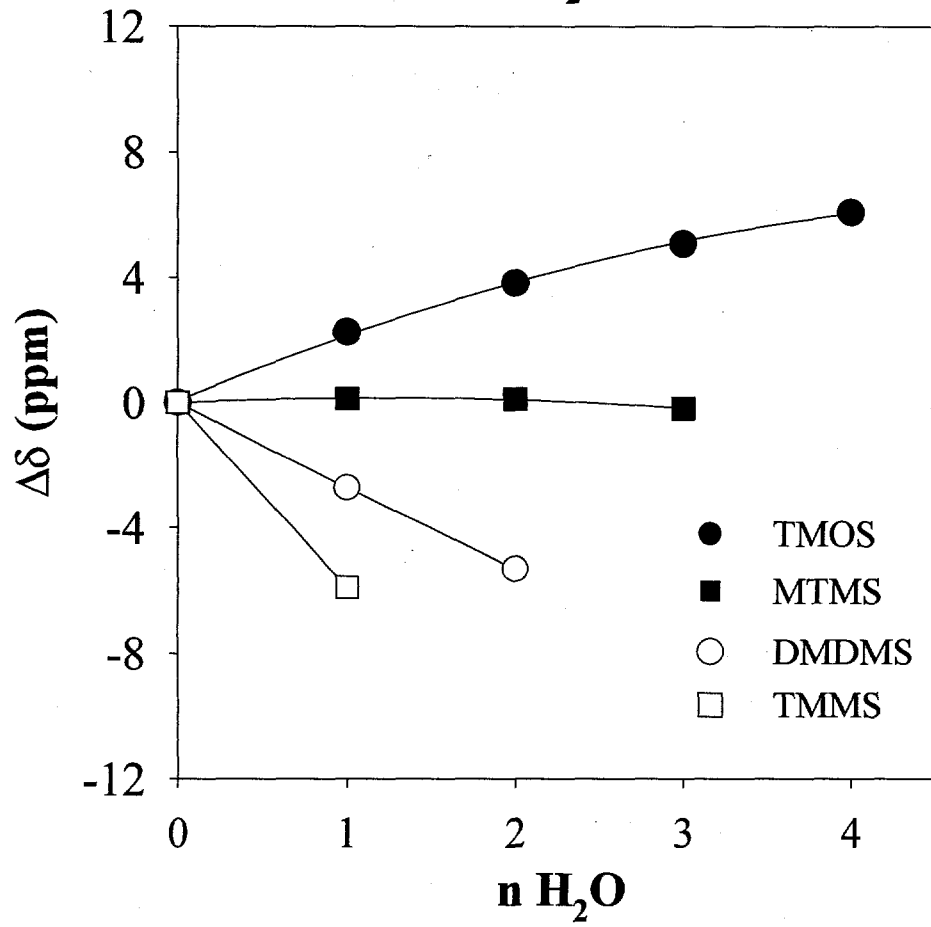
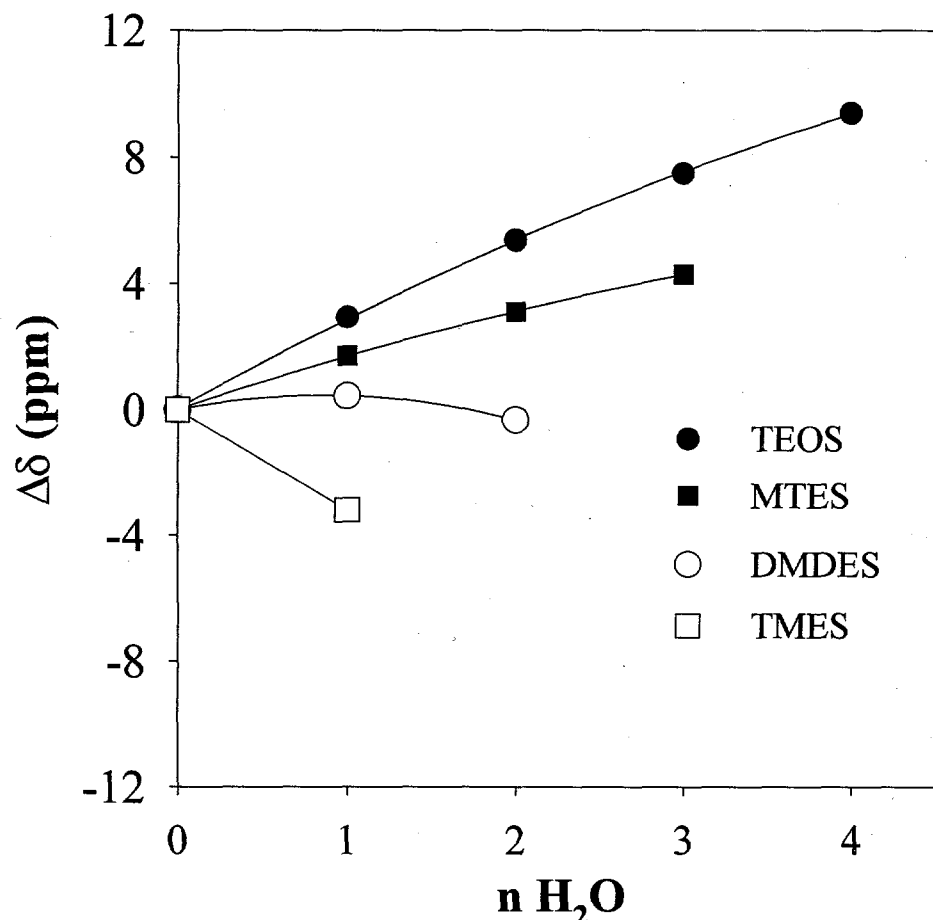
Table 5 Predicted PCM silicon outer valence gross population for the methyl alkoxy series

Compound	P_s	P_{xx}	P_{yy}	P_{zz}	ΔP	P_u
$\text{Si}(\text{OEt})_4$	1.28161	0.63487	0.63562	0.63977	0.00453	0.86805
$\text{Si}(\text{OEt})_3(\text{OH})$	1.25959	0.63625	0.63880	0.65151	0.01399	0.87199
$\text{Si}(\text{OEt})_2(\text{OH})_2$	1.23096	0.64229	0.64423	0.65252	0.00926	0.87494
$\text{Si}(\text{OEt})(\text{OH})_3$	1.18855	0.64780	0.64894	0.65291	0.00454	0.87742
$\text{Si}(\text{OH})_4$	1.11167	0.65684	0.65689	0.65727	0.00041	0.88235
$\text{MeSi}(\text{OEt})_3$	1.29062	0.63039	0.66989	0.76864	0.11850	0.90537
$\text{MeSi}(\text{OEt})_2(\text{OH})$	1.26435	0.63632	0.67676	0.78021	0.12367	0.91049
$\text{MeSi}(\text{OEt})(\text{OH})_2$	1.23506	0.63875	0.67962	0.78246	0.12327	0.91199
$\text{MeSi}(\text{OH})_3$	1.19168	0.63272	0.67579	0.78347	0.12921	0.91040
$\text{Me}_2\text{Si}(\text{OEt})_2$	1.29475	0.63220	0.71041	0.90664	0.23534	0.94404
$\text{Me}_2\text{Si}(\text{OEt})(\text{OH})$	1.27490	0.63123	0.71065	0.91622	0.24528	0.94605
$\text{Me}_2\text{Si}(\text{OH})_2$	1.24441	0.62382	0.70807	0.91936	0.25342	0.94544
$\text{Me}_3\text{Si}(\text{OEt})$	1.30834	0.74273	0.74349	0.91885	0.17574	0.96411
$\text{Me}_3\text{Si}(\text{OH})$	1.29209	0.73207	0.73215	0.92441	0.19231	0.96258
$\text{Si}(\text{OMe})_4$	1.24914	0.64468	0.64468	0.64468	0.00000	0.87375
$\text{Si}(\text{OMe})_3(\text{OH})$	1.22700	0.64479	0.64614	0.65147	0.00601	0.87572
$\text{Si}(\text{OMe})_2(\text{OH})_2$	1.19741	0.65042	0.65090	0.65217	0.00151	0.87831
$\text{Si}(\text{OMe})(\text{OH})_3$	1.16670	0.65011	0.65142	0.65549	0.00472	0.87914
$\text{MeSi}(\text{OMe})_3$	1.26228	0.63836	0.67785	0.78441	0.12630	0.91203
$\text{MeSi}(\text{OMe})_2(\text{OH})$	1.24268	0.63876	0.68100	0.78841	0.12854	0.91361
$\text{MeSi}(\text{OMe})(\text{OH})_2$	1.22737	0.62933	0.67436	0.78694	0.13510	0.91031
$\text{Me}_2\text{Si}(\text{OMe})_2$	1.27707	0.63823	0.71782	0.91679	0.23877	0.94811
$\text{Me}_2\text{Si}(\text{OMe})(\text{OH})$	1.25994	0.63639	0.71570	0.92427	0.24823	0.94919
$\text{Me}_3\text{Si}(\text{OMe})$	1.29719	0.74733	0.74813	0.91863	0.17090	0.96510
Me_4Si	1.32852	0.85032	0.85032	0.85032	0.00000	0.97760

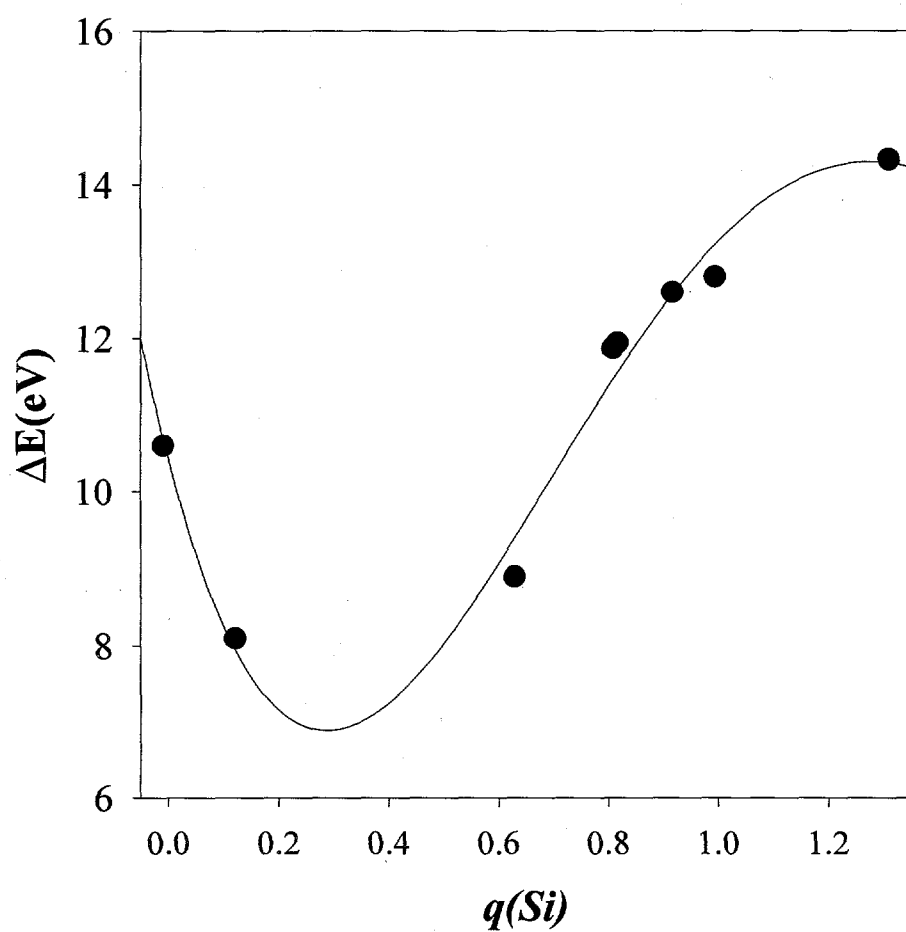
Table 6 ^{29}Si NMR shielding constants and corresponding parameters for methyl alkoxy series

Compound	σ_{exp} (ppm)	σ_{iso} (ppm) ^a	σ_{dia} (ppm)	q(Si)	ΔE	$\Delta\sigma$ (ppm)	η
Si(OEt) ₄	450.72	450.97 (+0.25)	1068.28	0.808	11.87	1.17	0.25
Si(OEt) ₃ (OH)	447.38	447.96 (+0.58)	1068.12	0.814	11.90	3.60	0.26
Si(OEt) ₂ (OH) ₂	444.95	445.43 (+0.48)	1067.74	0.830	12.00	2.35	0.31
Si(OEt)(OH) ₃	443.24	443.08 (-0.16)	1067.01	0.862	12.22	1.14	0.37
Si(OH) ₄	440.82	440.79 (-0.03)	1066.87	0.917	12.60	0.10	0.00
MeSi(OEt) ₃	412.56	412.75 (+0.19)	1053.19	0.640	10.85	29.05	0.33
MeSi(OEt) ₂ (OH)	408.93	408.93 (-0.00)	1053.04	0.642	10.86	29.76	0.32
MeSi(OEt)(OH) ₂	407.53	406.90 (-0.63)	1052.60	0.664	11.01	29.45	0.32
MeSi(OH) ₃	406.93	406.80 (-0.13)	1052.63	0.716	11.31	31.36	0.32
Me ₂ Si(OEt) ₂	374.07	374.10 (+0.03)	1038.28	0.456	9.71	53.35	0.14
Me ₂ Si(OEt)(OH)	371.91	372.27 (+0.36)	1038.08	0.467	9.78	55.69	0.13
Me ₂ Si(OH) ₂	372.44	372.05 (-0.39)	1038.09	0.504	10.02	58.39	0.12
Me ₃ Si(OEt)	353.84	353.39 (-0.45)	1023.21	0.287	8.73	31.36	0.00
Me ₃ Si(OH)	353.43	352.32 (-1.11)	1024.04	0.319	8.91	35.95	0.00
Si(OMe) ₄	447.31	446.55 (-0.76)	1067.98	0.817	11.94	0.00	0.00
Si(OMe) ₃ (OH)	444.53	444.81 (+0.28)	1067.69	0.831	12.01	1.52	0.33
Si(OMe) ₂ (OH) ₂	442.96	442.57 (-0.39)	1067.25	0.849	12.14	0.37	0.47
Si(OMe)(OH) ₃	441.72	441.71 (-0.01)	1066.66	0.876	12.32	1.17	0.41
MeSi(OMe) ₃	408.61	407.98 (-0.63)	1053.06	0.637	10.84	30.27	0.30
MeSi(OMe) ₂ (OH)	406.61	406.34 (-0.27)	1052.83	0.649	10.91	30.62	0.31
MeSi(OMe)(OH) ₂	406.63	407.46 (+0.83)	1052.41	0.682	11.09	32.96	0.31
Me ₂ Si(OMe) ₂	370.48	371.33 (+0.85)	1038.25	0.450	9.66	52.96	0.13
Me ₂ Si(OMe)(OH)	369.96	370.07 (+0.11)	1038.02	0.464	9.76	55.48	0.11
Me ₃ Si(OMe)	351.18	352.10 (+0.92)	1022.84	0.289	8.72	29.96	0.00
Me ₄ Si	368.50	368.55 (+0.05)	1008.13	0.121	8.10	0.00	0.00

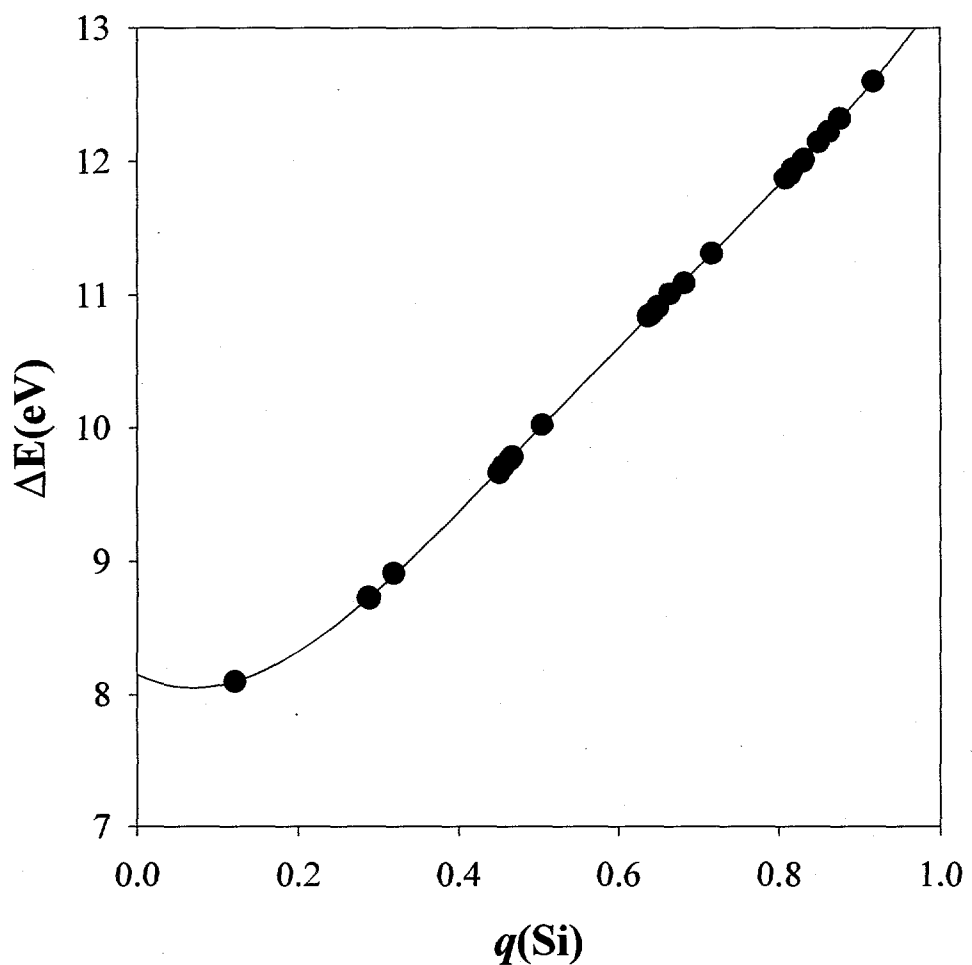
^a Error between experiment and theory given in parenthesis.



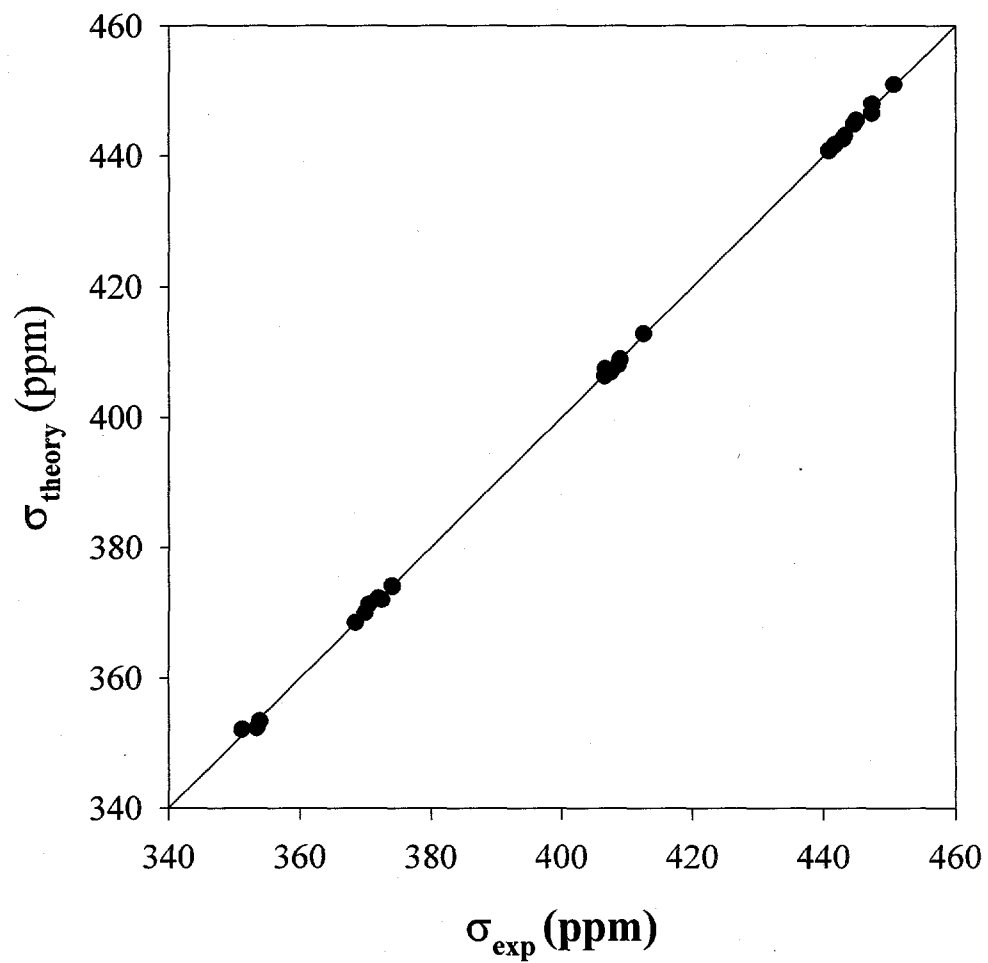
Alam and Henry, Fig. 1



Alam and Henry Fig. 2



Alam and Henry Fig. 3



Alam and Henry Fig. 4